

1 **Spatio-temporal assessment of annual water-balance model for Upper Ganga** 2 **Basin**

3 Anoop Kumar Shukla¹, Shray Pathak¹, Lalit Pal¹, Chandra Shekhar Prasad Ojha¹, Ana Mijic²,
4 Rahul Dev Garg¹

5 ¹Department of Civil Engineering, Indian Institute of Technology Roorkee, Uttarakhand, India

6 ²Department of Civil and Environmental Engineering, Imperial College London, London, UK

7 E-mail- anoopgeomatics@gmail.com, shraypathak@gmail.com, lalitpl4@gmail.com,
8 cspojha@gmail.com, ana.mijic@imperial.ac.uk, rdgarg@gmail.com

9 **Abstract**

10 The Upper Ganga Basin, Uttarakhand, India has high hydropower potential and plays an important
11 role in development of state economy. Thus, knowledge about water yield is of paramount
12 importance to this region. The paper deals with use of contemporary water yield estimation
13 models, such as the distributed model (InVEST), Lumped Zhang model and their validation to
14 identify the most suited one for water yield estimation in this region. Earlier, while utilizing these
15 models, attempts were made to consider a single value of some important model parameters which
16 in fact show a variation at a pixel level scale. Therefore, in this study, the pixel level computations
17 are performed to assess and ascertain their need in model applications. To validate the findings,
18 the observed sub-basin discharge data is analyzed with the computed water yield for four decades,
19 i.e. 1980, 1990, 2001 and 2015. The results obtained are in good agreement with the water yields
20 obtained at pixel scale.

21 **Keywords:** Ecosystem, Evapotranspiration, Water Yield, Lumped Zhang model, InVEST model

22 **1. Introduction**

23 Accurate assessment of key ecosystem services (ES) such as water yield have gained focus in
24 recent years in ecosystem service modelling as fresh water availability in a region are essential for
25 agriculture, industry, human consumption, hydropower, etc. (Readhead et al., 2016). Hydrological
26 ecosystem services often include drinking waters supply, power production, industrial use,
27 irrigation, and many more. These hydrological ES are dependent on different factors such as
28 watershed characteristics (e.g. topography, land use land cover (LULC), soil type) and climatic
29 condition. To incorporate these concepts into assessment and decision making, there has been a
30 proliferation of ecosystem modelling tools and methods. Models for ecosystem services valuation
31 often focus on using globally available data, accepting large number of spatially explicit inputs
32 and producing spatially explicit output, and limiting the model structure to key biophysical
33 processes involved in land-use change (Guswa et al. 2014). Precise estimation of ES using these
34 models is a complicated task owing to spatial variability and dependence of ES on various
35 topographical and climatic factors. Further validation and uncertainty assessment in model output
36 have proven to be a key obstacle to the application ES models. In the literature, studies focusing
37 on comparison of different ES models have projected some light over the model output validation
38 issues, however, there still exist lack of studies highlighting validation of these models for Indian
39 basins. Further, the benefits that can be derived from ES should be analyzed and quantified in a
40 spatially explicit manner (Sanchez et al. 2012). The uncertainties in the determination of spatial
41 and temporal distribution of the climatic variables, especially precipitation constitutes a major
42 obstacle to the understanding of hydrological behaviour at the catchment scales (Milly et al. 2002).
43 The Integrated Valuation of Ecosystem Services and Tradeoffs (InVEST) model, developed by
44 Natural Capital Project (Tallis et al. 2010) is a tool which provides a framework to planners and

45 decision makers to assess trade-offs among ecosystem services and enables their comparison in
46 various climate and land use change scenarios. It includes a biophysical component, computing
47 the provision of freshwater or water yield, by different parts of the landscape and a valuation
48 component, representing the benefits of water provisioning to people. This model works on
49 simplified Budyko theory, which has a long history and still continues to receive interest in the
50 hydrological literature (Budyko 1979; Zhou et al. 2012; Zhang et al. 2004; Ojha et al. 2008; Zhang
51 et al. 2001; Donohue et al. 2012; Xu et al. 2013; Wang et al. 2014). The InVEST model applies a
52 one-parameter formulation of the theory in a semi-distributed way (Zhang et al. 2004). The model
53 is capable of quantifying water yield of a catchment under the influence of change in drivers viz.
54 climate variable and catchment characteristics (e.g. land use change). Various studies have been
55 carried out in the past demonstrating application of InVEST model. Sanchez-Canales et al. (2012)
56 carried out sensitivity analysis of three parameters i.e. z (seasonal precipitation coefficient),
57 precipitation (annual) and ET_0 (annual reference precipitation) using the InVEST model for a
58 Mediterranean region basin and found precipitation to be the most sensitive parameter for the study
59 region. Later, Terrado et al. (2014) applied the InVEST model for the heavily humanized Llobregat
60 river basin. The model is applied for both extreme wet and dry conditions and the role of climatic
61 parameters is emphasized. Hoyer et al. (2014), applied this model in Tualatin and Yamhill basins
62 of northwestern Oregon under the series of urbanization and climate change scenarios. The results
63 show that the climatic parameters have more sensitivity than other inputs for a water yield model.
64 Hamel et al. (2014), applied the same water yield model for the Cape Fear catchment, North
65 Carolina and concluded that the precipitation is the most influencing parameter. Goyal et al. (2017)
66 analyzed the InVEST water yield model for the hilly catchment by taking two catchments i.e.
67 Sutlej river catchment and Tungabhadra river catchment. The climate parameters i.e. precipitation

68 and ET_0 are observed to be most influencing parameters. However, there exist certain factors
69 limiting the application of InVEST models such as the absence or inadequate comparison with
70 observed data, calibration of the model without prior identification of sensitive parameters, and
71 lack of validation of the predictive capabilities in the context of Land Use Land Cover change (Bai
72 et al. 2012; Nelson et al. 2010; Su et al. 2013; Terrado et al. 2014).

73 The InVEST model operates on the principle of Budyko theory (Budyko, 1958, 1974). Based on
74 works of Schreiber (1904) and Ol'Dekop (1911), Budyko proposed formulations explaining the
75 relationship between precipitation and potential evapotranspiration (PET) in order to couple water
76 and energy balances, defined as Budyko hypothesis. Several attempts have been made to obtain
77 an analytical solution of the Budyko hypothesis (Schreiber, 1904; Ol'Dekop, 1911; Turc, 1954;
78 Mezentsev, 1955; Pike, 1964; Fu, 1981; Choudhury, 1999; Zhang et al., 2001, 2004; Porporato et
79 al., 2004; Yang et al., 2008; Donohue et al., 2012; Wang and Tang, 2014; Zhou et al., 2015).
80 Among these approaches, solutions provided by Fu (1981), called Fu's equation gained attention
81 as the work represented the effect of catchment properties on water balance components by
82 incorporating an addition parameter 'w'. Fu's equation can provide a full picture of the evaporation
83 mechanism at the annual timescale. Therefore, Fu's equation could be used through top-down
84 analysis for providing an insight into the dynamic interactions among climate, soils, and vegetation
85 and their controls on the annual water balance at the regional scale (Yang et al., 2007).

86 Considering the lack of studies on analysis and validation of ES in Indian sub-continent especially
87 for Himalayan catchments and to assess the applicability of various water-balance model to
88 Himalayan catchments, the present work attempts to compute and analyse water yield in Upper
89 Ganga basin using InVEST model. The work primarily considers in detail, the spatial variation of
90 InVEST model parameters and uses different strategies to compute water yield. Accordingly,

91 water yield is estimated for four years i.e. 1980, 1990, 2001 and 2015 and the most appropriate
92 strategy is identified. The parameters that are computed at basins level scale in previous studies
93 are estimated at pixel scale in order to avoid the dependence of model parameters on size of the
94 catchment. In addition, pixel level estimations of water yield are expected to be accurate than
95 output obtained using conventional approach. The term ‘finer scale’ in the paper represents
96 incorporation of spatial variations through pixel level estimation of parameters involved in
97 InVEST model which are otherwise taken as lumped. The work also attempts to compare the
98 outcomes of spatially distributed water yield model and conventionally used lumped Zhang model.

99 **2. Background Theory**

100 ***2.1 Water Yield Models***

101 In this section, two water yield models, i.e. InVEST water yield model, which is a distributed
102 model and Lumped Zhang model are described.

103 ***2.1.1 InVEST model***

104 The InVEST water yield model (Tallis *et al.* 2010) is designed to provide the information regarding
105 the changes in the ecosystem that are likely to alter the flows. It is based upon the Budyko theory
106 which is an empirical function that yields the ratio of actual to potential evapotranspiration
107 (Budyko, 1979). To describe the degree to which long-term catchment water-balances deviate
108 from the theoretical limits, a number of scholars have proposed one-parameter functions that can
109 replicate the Budyko curve (Fu 1981, Choudhury 1999, Zhang *et al.* 2004, Wang *et al.* 2014). To
110 observe and represent pixel-level changes to the landscape, InVEST model incorporates explicitly
111 the spatial variability in precipitation and PET, soil depth and vegetation. The model operates at
112 grid scale and acquires the inputs in the raster format into a GIS environment such as ArcGIS.

113 The InVEST water yield model is based on an empirical function known as the Budyko curve
 114 (Budyko 1974). Water yield $Y(x)$ is determined for each pixel annually for a landscape as follows:

$$115 \quad Y(x) = \left(1 - \frac{AET(x)}{P(x)}\right) \times P(x) \quad (1)$$

116 where, $AET(x)$ is the actual annual evapotranspiration per pixel x ; and $P(x)$ is the annual
 117 precipitation per pixel x . Actual evapotranspiration (AET) is essentially determined by climate
 118 factors (precipitation, temperature, etc.) and mediated by catchment characteristics (vegetation
 119 cover, soil characteristics, topography, etc.). On the other hand, potential evapotranspiration (PET)
 120 represents the evaporating potential of the climate system prevail at a specific location and time of
 121 year without the consideration of catchment characteristics and soil properties (Allen et al., 1998).
 122 Several attempts have been made in past to establish relationship between AET and PET, among
 123 which solution provided by Fu (1981) are adopted worldwide. Fu (1981) provided an analytical
 124 solution to the Budyko hypothesis and related AET with PET by incorporating a dimensionless
 125 parameter ‘ w ’ which denotes the effect of catchment characteristics.

126 The InVEST model uses the expression of the Budyko curve proposed by Fu (1981) and Zhang *et*
 127 *al.* (2004). The ratio of mean annual potential evapotranspiration to annual precipitation, known
 128 as index of dryness, is expressed as:

$$129 \quad \frac{AET(x)}{P(x)} = 1 + \frac{PET(x)}{P(x)} - \left[1 + \frac{PET(x)}{P(x)}\right]^{\left(\frac{1}{w}\right)} \quad (2)$$

130 where, $PET(x)$ is the annual potential evapotranspiration per pixel x (mm); and $w(x)$ is a non-
 131 physical parameter that influences the natural climatic soil properties. The $PET(x)$ is calculated
 132 using the following expression:

$$133 \quad PET(x) = Kc(x) \times ETo(x) \quad (3)$$

134 where, $ET_o(x)$ is the annual reference evapotranspiration per pixel x which is calculated based
 135 on evapotranspiration of grass of alfalfa grown at that location shown in the equation (6). $K_c(x)$
 136 is the vegetation evapotranspiration coefficient that is influenced by the change in characteristics
 137 of land use land cover for every pixel (Allen et al. 1998). The values of $ET_o(x)$ are adjusted by
 138 $K_c(x)$ for each pixel over the land use land cover map. $w(x)$ is an empirical parameter and the
 139 expression given by Donohue et al. (2012) for the InVEST model has been applied to define $\omega(x)$
 140 which is as follows:

$$141 \quad w(x) = z \times \frac{AWC(x)}{P(x)} + 1.25 \quad (4)$$

142 Thus, the minimum value of the parameter $w(x)$ is 1.25 corresponding to bare soil where root
 143 depth is zero (Donohue et al. 2012) . The Donohue model was developed for Australia, however,
 144 the online documentation on InVEST model states its application globally. The parameter z is
 145 known as seasonality factor whose values vary from 1 to 30. It represents the nature of local
 146 precipitation and other hydrogeological parameters. The parameter $AWC(x)$ depicts volumetric
 147 plant available water content which is expressed in depth (mm) which can be expressed by
 148 following formula for each pixel x :

$$149 \quad AWC(x) = Min. (Restricting\ layer\ depth, root\ depth) \times PAWC \quad (5)$$

150 Root restricting layer depth is defined as the depth of the soil upto which the soil can allow the
 151 penetration of roots and root depth is defined as the depth where 95 percent of the root biomass
 152 occurs. Plant Available Water Content (PAWC) is generally taken as the difference between the
 153 field capacity and wilting point. It depends upon the soil properties and can be computed by the
 154 Soil-Plant-Air-Water (SPAW) software. PAWC is calculated using the method described by

155 Mckenzie et al. (2003). Modified Hargreaves method and Hargreaves method were employed for
156 computing the reference evapotranspiration for the study area at pixel scale.

157 Modified Hargreaves method

$$158 \quad ET_o = 0.0013 \times 0.408 \times RA \times (T_{avg} + 17.0) \times (TD - 0.0123 \times P)^{0.76} \quad (6)$$

159 where, ET_o is reference evapotranspiration, T_{avg} is average daily temperature ($^{\circ}C$) defined as the
160 average of the mean daily maximum and mean daily minimum temperature, TD ($^{\circ}C$) is the
161 temperature range computed as the difference between mean daily maximum and mean daily
162 minimum temperature, and RA is extraterrestrial radiation expressed in [$MJm^{-2}d^{-1}$].

163 Hargreaves method

$$164 \quad ET_o = 0.0023 \times 0.408 \times RA \times (T_{avg} + 17.8) \times TD^{0.5} \quad (7)$$

165 where, ET_o is reference evapotranspiration, T_{avg} is average daily temperature ($^{\circ}C$) defined as the
166 average of the mean daily maximum and mean daily minimum temperature, TD ($^{\circ}C$) is the
167 temperature range computed as the difference between mean daily maximum and mean daily
168 minimum temperature, and RA is extraterrestrial radiation expressed in ($MJm^{-2}d^{-1}$).

169 For computing the extraterrestrial radiation (RA), following equation is used

$$170 \quad RA = \frac{24(60)}{\pi} \times G_{sc} \times d_r \times [w_s \sin(\varphi) \sin(\delta) + \cos(\varphi) \cos(\delta) \sin(w_s)] \quad (8)$$

171 where, RA is extraterrestrial radiation [$MJm^{-2}d^{-1}$], d_r is the inverse relative distance Earth-Sun, G_{sc}
172 is solar constant equals to $0.0820 MJm^{-2}min^{-1}$, w_s is sunset hour angle (rad), δ is solar declination
173 (rad) and φ is latitude (rad).

174 *Determination of Seasonality factor (z) parameter*

175 The seasonality factor (z) parameter varies depending upon the local precipitation patterns such as
176 the hydrological characteristics of the area, its rainfall intensity and topography. According to the
177 InVEST water yield model (Tallis et al. 2010), parameter z can be computed in three different
178 ways. First method is suggested by Donohue *et al.* (2012), in which parameter z is expressed as
179 the one fifth of the number of rain events per year. Second method is suggested by Xu *et al.* (2013),
180 which relates $\omega(x)$ with latitude, NDVI (Normalized Difference Vegetation Index), area, etc.
181 Third method experiments with various selections of w (one value of w for the entire study region)
182 till there is a good match between observed and computed water yield. Unfortunately, this method
183 is not suited to a pixel based analysis as the number of pixels will be extremely large making the
184 method to be computationally intensive.

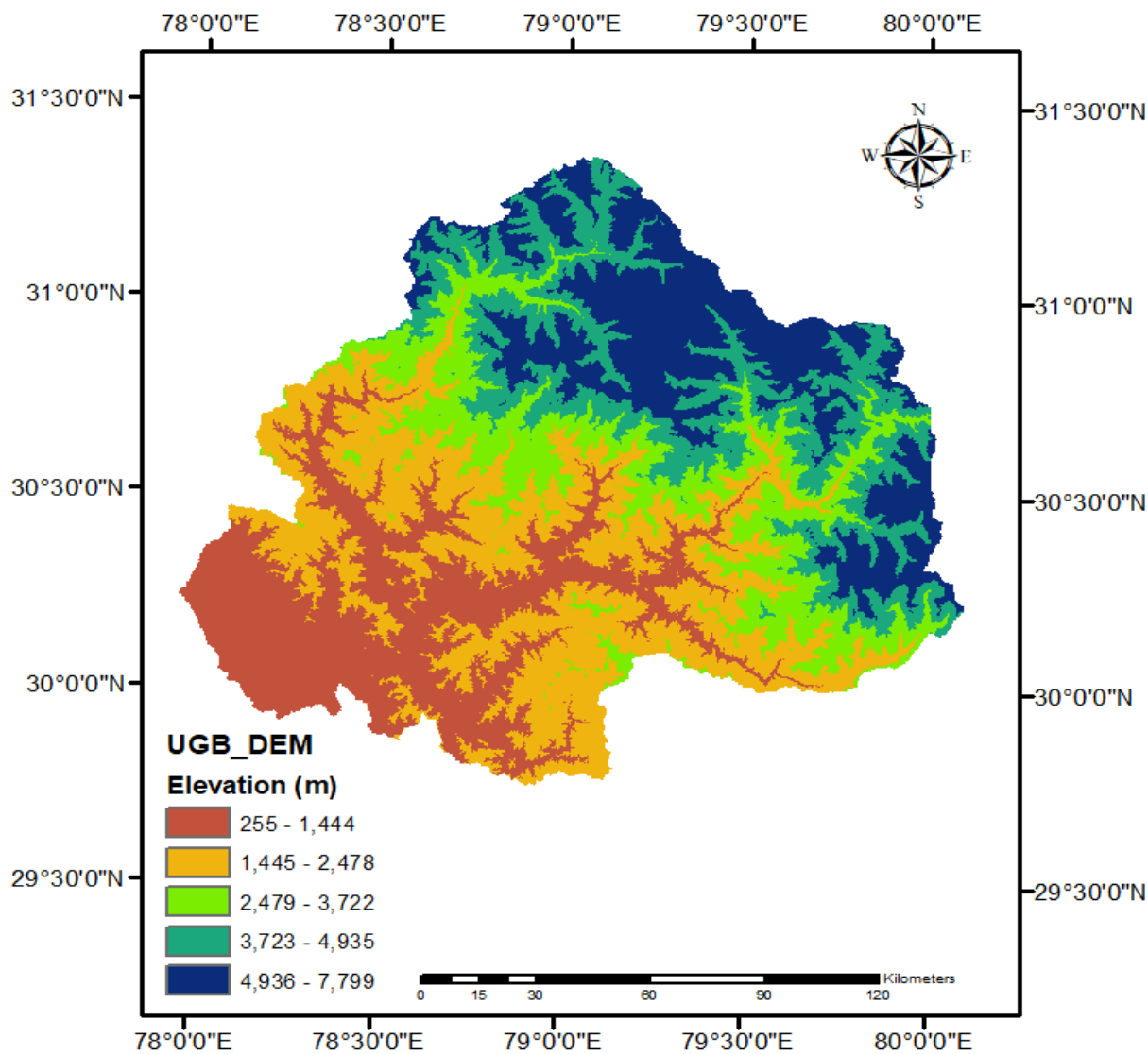
185 *2.1.2 Lumped Zhang model*

186 In this model all the mean values of the parameters are used as an input to compute the average
187 value of the water yield for the whole watershed. In this model the averaged actual transpiration,
188 potential evapotranspiration, w , precipitation is used as described by Zhang *et al.* (2004)

189 **3. Study Area**

190 The Ganga river in India is ranked amongst the world's top 20 rivers in regards to the flow
191 discharge. The Ganga river is segregated into three zones, viz., Upper Ganga basin, Middle Ganga
192 basin and Lower Ganga basin. The area chosen for the present study, i.e., Upper Ganga river
193 basin is situated in the northern part of India within the geographical coordinates $30^{\circ} 38'$ - $31^{\circ} 24'$
194 N latitude and $78^{\circ} 29'$ - $80^{\circ} 22'$ E longitude with an area of 22,292.1 km² upto Haridwar.. The
195 altitude of the study area varies from 7512 m in the Himalayan terrains to 275 m in the plains.
196 Approximately 433 km² of entire region of the basin is under glacier landscape and 288 km² is

197 under fluvial landscape. About 60% of the basin is utilized for agricultural, 20% of the basin is
198 under the forest area, especially in the upper mountainous region. Nearly 2% of the basin is
199 permanently covered with snow in the mountain peaks. Most predominant soil groups found in the
200 region are sand, clay, loam and their compositions. In the Upper Ganga river basin, the average
201 annual rainfall varies from 550 to 2500 mm (Bharati et al. 2011) and a major fraction of total
202 annual rainfall is received during monsoon months (June-September). The geographical location
203 and other information of the study area Upper Ganga river basin are represented in Fig. 1.



204

205

Figure 1. Graphical representation of study area, Upper Ganga basin

206 **4. Methodology**

207 **4.1 Data**

208 *4.1.1 Precipitation and Temperature*

209 The daily time series of precipitation and temperature for the study area is acquired from India
210 Meteorological Department (IMD) at a grid size of 0.25 degrees and 1 degree, respectively. The
211 Upper Ganga basin comes in the latitude ranging from 29.5 degrees to 31.5 degrees and longitude
212 ranging from 77.75 degrees to 80.25 degrees. The daily time series of precipitation was aggregated
213 to obtain the annual time series at each grid point. Various analysis in the study are carried out for
214 four years i.e. 1980, 1990, 2001 and 2015.

215 *4.1.2 Soil Map*

216 Spatial maps of soil were collected from National Bureau of soil survey and land use planning
217 (NBSSLUP) at 1:250000. Digital maps of soil available at a resolution of 1200m×1200m were
218 resampled to the resolution of land use data i.e. 30m×30m using ‘resample’ tool in ArcGIS in order
219 to maintain the scale homogeneity. The attribute table of the raster layer contains fields like soil
220 depth, soil texture, percentage carbon content, drainage, slope, erosion, soil temperature and
221 mineralogy. The relevant feature, i.e. of soil depth and soil texture are converted into the raster
222 image for the Upper ganga basin.

223 *4.1.3 LandUse/Land Cover map*

224 Satellite images were acquired from different sensors of Landsat viz. Landsat 3/4 MSS/TM,
225 Landsat 4 TM, Landsat 7 ETM and Landsat 8 OLI sensors for the year 1980, 1990, 2001 and 2015
226 respectively. The images are available at different resolution and for several bands out of which
227 Green (G), Red (R) and Near Infrared (NIR) band images are combined to create False Colour

228 Composite (FCC) for the study area in ERDAS Imagine. FCCs are then classified using supervised
 229 classification in ERDAS in six different classes, i.e. Forest, Water, Agricultural, Wasteland, Snow
 230 and Glacier and Built-up land. Classification of the area is based upon their similar response under
 231 different bands. Each class is then recognized with the help of ground truth and high resolution
 232 satellite images.

233 ***4.2 Methodology to compute water yield***

234 In the present work, five different strategies are employed to compute water yield..For the ease of
 235 presentation, these strategies are referred as A, B, C, D, E. In strategy A, an average value of
 236 precipitation, temperature, extraterrestrial radiation and parameter ‘w’ is used for the entire basin.
 237 This strategy is essentially based on Lumped Zhang Model. Strategies B, C, D and E are designated
 238 corresponding to particular variation of InVEST model where water yield is computed using
 239 different approach for estimating ‘w’ parameter. For computing parameter ‘w’, Xu et al. (2013)
 240 relationship for large basin and global level is given by equation (9) and equation (10) respectively.

241 *For Large basins:*

$$242 \quad w = 0.69387 - 0.01042 \times lat + 2.81063 \times NDVI + 0.146186 \times CTI \quad (9)$$

243 *For global model:*

$$244 \quad w = 3.50412 - 0.09311 \times slp - 0.03288 \times lat + 1.12312 \times NDVI - 0.00205 \times long -$$

$$245 \quad 0.00026 \times elev \quad (10)$$

246 where, *slp* is slope gradient, *lat* is absolute latitude of basin center, *CTI* is compound topographic
 247 index, *NDVI* is normalized difference vegetation index, *long* is longitude and *elev* is elevation.

248 In strategy B, entire basin is considered for computing the parameter 'w' for large basins (equation
249 9) by Xu et al. (2013). In strategy C, entire basin is considered for computing the parameter 'w'
250 for Global model (equation 10) by Xu et al. (2013). In strategy D, parameter 'w' is computed at
251 each pixel in order to incorporate the spatial distribution of the hydrologic variables involved in
252 the computations. In Strategy E, parameter 'z' is computed according to the number of rain events
253 in a year and subsequently equation (4) is used to compute the parameter 'w'.

254 For all the strategies, extraterrestrial radiation (RA) parameter is computed for each month using
255 equation (8) and a raster layer is generated. Precipitation data is obtained from Indian
256 Meteorological Department (IMD) at grid size of 0.25 degree for the study area and has been
257 interpreted and converted to raster format by using Inverse Distance Weighted (IDW) interpolation
258 technique in ArcGIS environment for obtaining the values for all pixels at a resolution equal to the
259 resolution of the Landsat satellite image The temperature dataset is obtained from IMD at grid size
260 of $1^{\circ} \times 1^{\circ}$ for the study area and has been interpreted and converted to raster format by using IDW
261 interpolation technique for obtaining the values for all pixels at a resolution equal to the resolution
262 of the Landsat satellite images. Subsequently, the mean monthly value of average temperature
263 (Tavg) and the difference between mean daily maximum and mean daily minimum (TD) is
264 obtained. The climate datasets used in the present study are of the finest resolution available so far
265 for the study region. The precipitation and temperature data sets were downscaled to a resolution
266 of land use data using Spline interpolation technique. Gridded datasets of temperature and
267 precipitation used in the present study has been developed using quality controlled stations and
268 well-proven interpolation technique. Further details about the datasets are given in Srivastava et
269 al. (2009) and Pai et al. (2014).

270 Modified Hargreaves method is applied for obtaining the values of reference evapotranspiration at
 271 each pixel for each month (Droogers et al. 2002). In this method, the inputs are R_a , precipitation,
 272 T_{avg} and TD. Some of the months, i.e. July 1980, July 1990, August 1990, June 2001, July 2001,
 273 August 2001, June 2015, July 2015 and August 2015 showed the negative values of reference
 274 evapotranspiration as obtained from Modified Hargreaves method. Thus, for the above months the
 275 Hargreaves method as recommended by Droogers et al. (2002) is applied for obtaining the positive
 276 values for the reference evapotranspiration. Thus, all the mean values for the month are added up
 277 to get the mean yearly values for the year 1980, 1990, 2001 and 2015. To computed potential
 278 evapotranspiration, the yearly values obtained for the reference evapotranspiration have been
 279 multiplied by the vegetation evapotranspiration coefficient (K_c) which varies with the LULC
 280 characteristics as expressed in equation (3). The value of the vegetation evapotranspiration
 281 coefficient is taken from Allen *et al.* (1998) as shown in Table 1. In this study, K_c is taken same
 282 for all the four years from Table. 1 and is used to obtain potential evapotranspiration which is
 283 subsequently used to obtain the yearly potential evapotranspiration at each pixel of the study area.

284 **Table 1.** Value of K_c corresponding to LandUse/LandCover classes

S.No.	LandUse/LandCover	Percentage cover (1980)	Percentage cover (1990)	Percentage cover (2001)	Percentage cover (2015)	K_c
1	Forest	17.84	16.32	15.78	15.19	1
2	Water	21.87	21.27	19.47	17.65	1
3	Wastelands	51.1	52.36	54.18	55.46	0.2
4	Built-up Area	2.07	2.14	2.27	2.49	0.4
5	Agricultural	3.67	4.04	3.76	4.22	0.75

6	Snow and Glacier	3.45	3.87	4.54	4.99	2
---	------------------	------	------	------	------	---

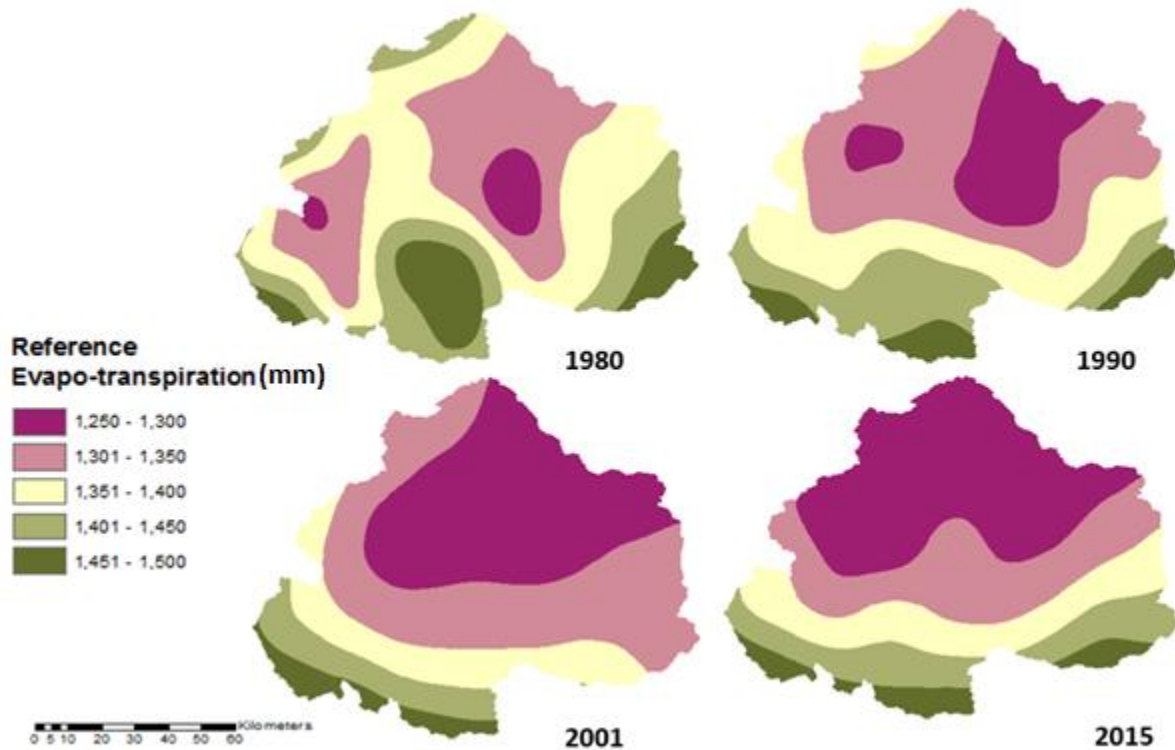
285

286 **5. Results**

287 **5.1 Reference Evapotranspiration, $ETo(x)$**

288 Reference Evapotranspiration is computed for the upper Ganga Basin using a high-resolution
 289 monthly climate dataset. Modified Hargreaves method is applied for obtaining the values of
 290 reference evapotranspiration at each pixel for each month (Droogers et al. 2002). The reference
 291 evapotranspiration is a function of R_E , precipitation, T_{avg} and TD which are already computed
 292 pixel wise for each month for the year 1980, 1990, 2001 and 2015.

293 Some of the months i.e. July 1980, July 1990, August 1990, June 2001, July 2001, August 2001,
 294 June 2015, July 2015 and August 2015 showed negative values of reference evapotranspiration on
 295 applying Modified Hargreaves method. Thus, for the above months, the Hargreaves method is
 296 applied for obtaining the positive results. Hence, all the mean values for the months are added up
 297 to get the mean yearly values of evapotranspiration for the years 1980, 1990, 2001 and 2015, as
 298 represented in Fig 2.

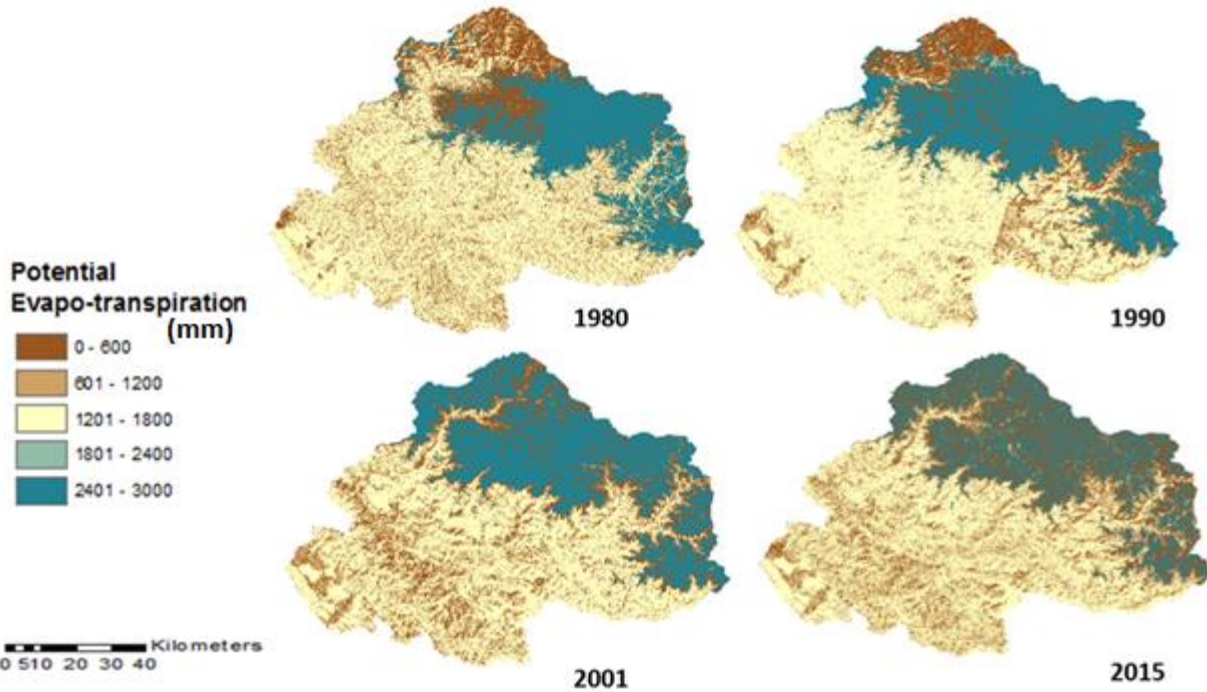


299

300 **Figure 2.** Reference Evapotranspiration (mm) of Upper Ganga Basin for the years 1980, 1990,
 301 2001 and 2015.

302 **5.2 Potential Evapotranspiration, $PET(x)$**

303 The annual values obtained for the reference evapotranspiration is multiplied by the vegetation
 304 evapotranspiration coefficient (K_c) which varies with the Land Use Land Cover characteristics, as
 305 expressed in equation (3). The value of the vegetation evapotranspiration coefficient is taken from
 306 Allen et al. (1998). The values of the vegetation evapotranspiration coefficient are taken from the
 307 Table 1. Thus, the potential evapotranspiration is computed for Upper Ganga Basin for the years
 308 1980, 1990, 2001 and 2015 as represented in Fig. 3.



309
 310 **Figure 3.** Potential Evapotranspiration (mm) of Upper Ganga Basin for the years 1980, 1990, 2001
 311 and 2015.

312 **5.3 Water Yield, $Y(x)$**

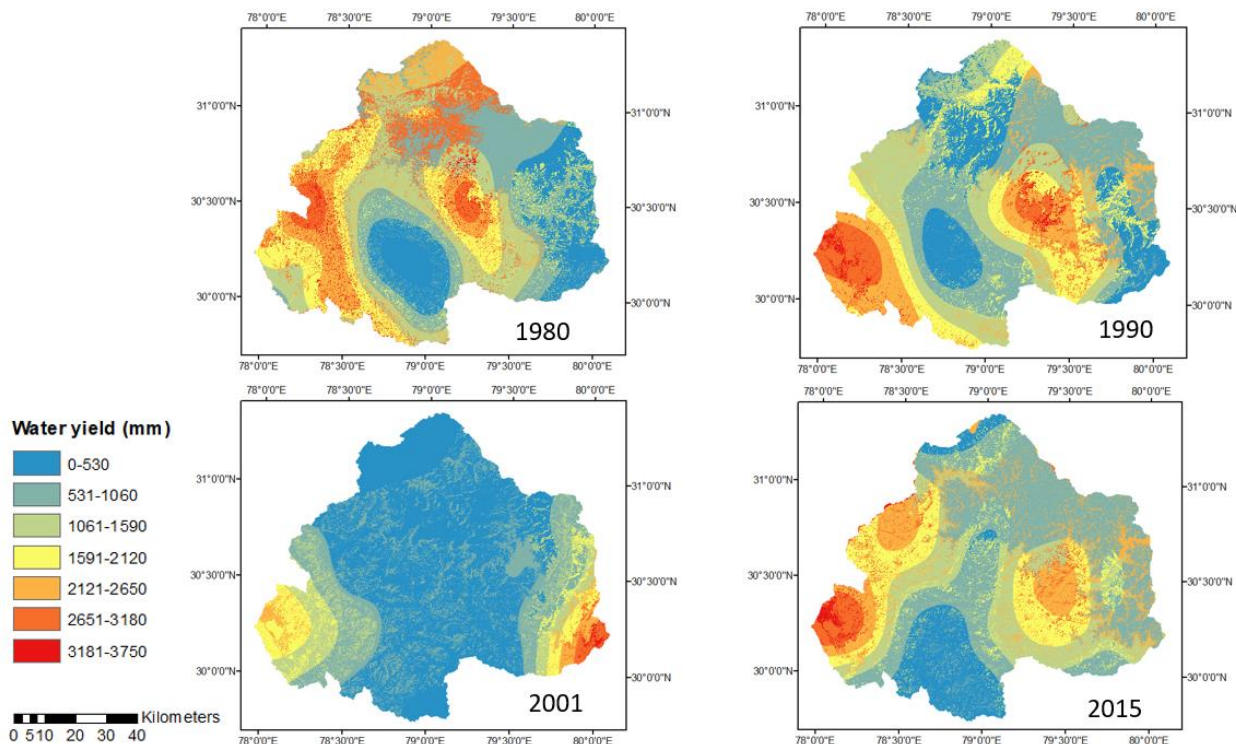
313 As mentioned in the methodology, the water yield for the Upper Ganga basin are computed using
 314 five strategies A, B, C, D and E:

315 ***Strategy A: Water yield computed using Lumped Zhang Model***

316 Here, the basin average values of all the input parameters are considered and the water yield is
 317 computed for the Upper Ganga basin for the year 1980, 1990, 2001 and 2015 which are obtained
 318 as 658.52 mm, 925.68 mm, 603.71 mm and 1194.25 mm, respectively.

319 ***Strategy B: Water yield obtained by taking the single weighted mean value of parameter ‘w’***
 320 ***from Xu et al. (2013) for Large basins.***

321 By considering a single value of the parameter ‘w’ for the whole basin the water yield is computed
 322 for Upper Ganga basin (equation 9). The weighted mean value for the parameter ‘w’ for the years
 323 1980, 1990, 2001 and 2015 are obtained as 1.507, 1.541, 1.403 and 1.507 respectively. The spatial
 324 distribution of water yield for the Upper Ganga basin for different years are represented in Fig. 4.
 325 The mean values of water yield as obtained using this method for the year 1980, 1990, 2001 and
 326 2015 are 755.65 mm, 959.48 mm, 742.39 mm and 1131.42 mm respectively.

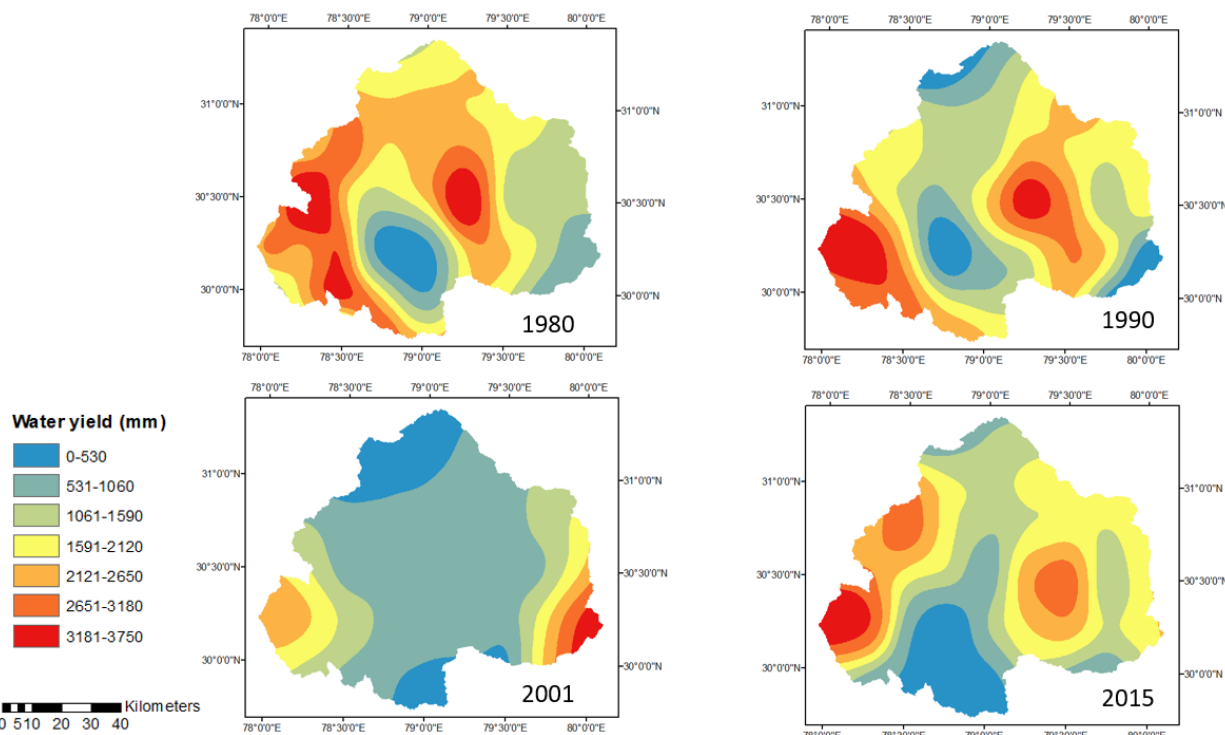


327 **Figure 4.** Water yield obtained by taking the single weighted mean value of parameter ‘w’ from
 328 Xu et al. (2013) for large basins.
 329

330 *Strategy C: Water yield obtained by taking the single weighted mean value of parameter ‘w’*
 331 *from Xu et al. (2013) for global model.*

332 By considering a single value of the parameter ‘w’ for the whole basin the water yield is computed
 333 for Upper Ganga basin (equation 10). The weighted mean value for the parameter ‘w’ for the years

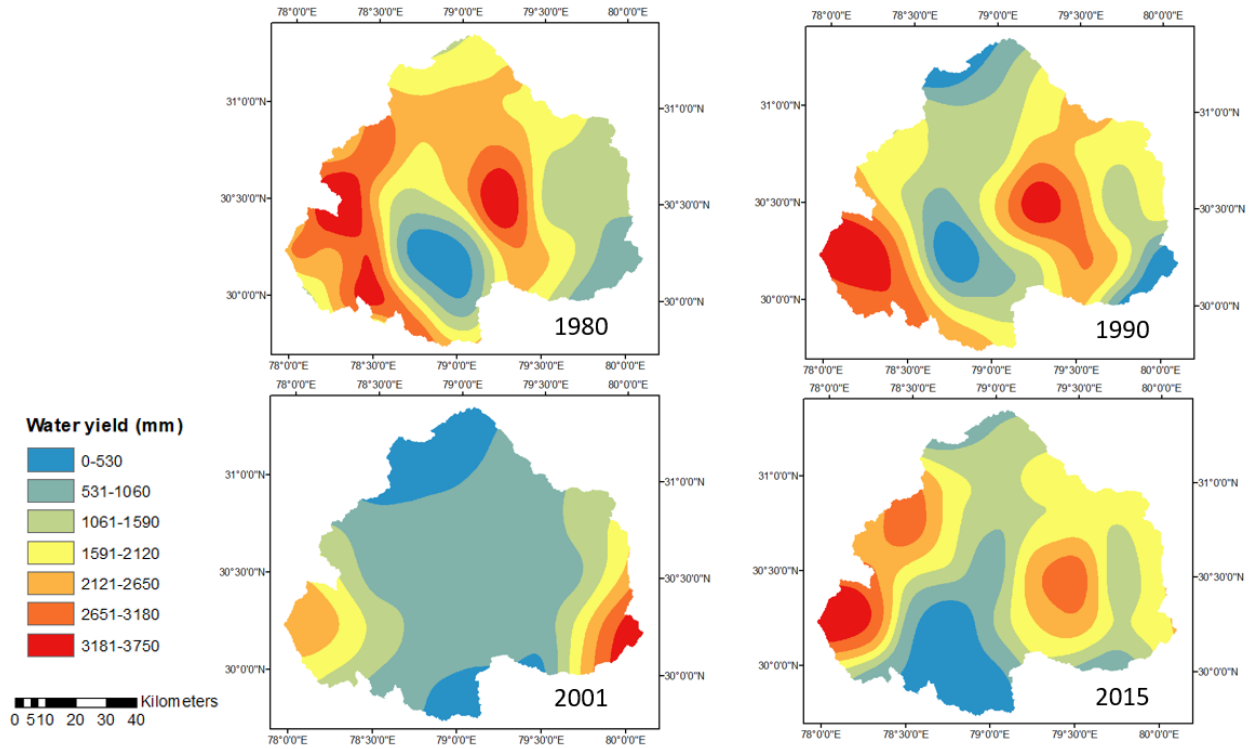
334 1980, 1990, 2001 and 2015 are obtained as -0.967, -0.955, -1.010 and -0.968 respectively. The
 335 spatial distribution of water yield for the Upper Ganga basin for the years are shown in Fig. 5. The
 336 mean values of water yield for the year 1980, 1990, 2001 and 2015 are 1239.92 mm, 1549.46 mm,
 337 1149.93 mm and 1754.59 mm respectively.



338
 339 **Figure 5.** Water yield obtained by taking the single weighted mean value of parameter “w” from
 340 Xu et al. (2013) for global model.

341 *Strategy D: Water yield obtained using pixel level estimation of parameter ‘w’ from Xu et al.*
 342 *(2013)*

343 In this strategy, the values of parameter ‘w’ is computed at pixel level. The water yield computed
 344 for the years 1980, 1990, 2001 and 2015 for the Upper Ganga Basin are represented in Fig. 6. The
 345 mean values of water yield for the year 1980, 1990, 2001 and 2015 are 1240.02 mm, 1549.44 mm,
 346 1149.89 mm and 1754.62 mm respectively.

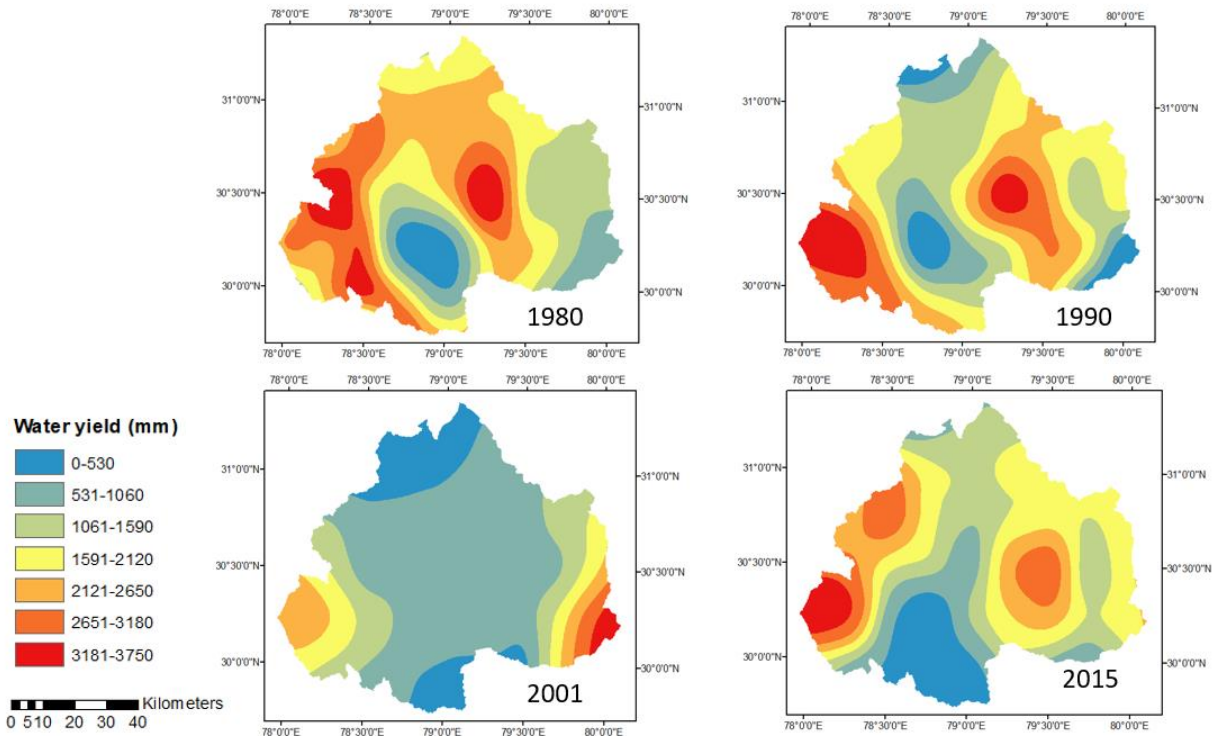


347

348 **Figure 6.** Water yield obtained by computing pixel wise value of parameter “w” from Xu et al.
 349 (2013)

350 *Strategy E: Water yield obtained using pixel level estimation of parameter ‘w’ from Donohue et*
 351 *al. (2012)*

352 The equation (4), represents the parameter ‘w’ which is a function of the parameters ‘z’, AWC and
 353 P. The parameter ‘w’ in the equation involved in strategy ‘E’ have been proposed by Donohue et
 354 al. (2012) which is also cited in online documentation of InVEST model, however, the final
 355 equation used for estimating water yield is from the InVEST model. Considering this fact,
 356 Donohue et al. (2012) has been cited in Strategy ‘E’. The water yield is computed for Upper Ganga
 357 Basin for the years are shown in Fig. 7. The mean values of water yield for the years 1980, 1990,
 358 2001 and 2015 are 1241.09 mm, 1552.38 mm, 1153.95 mm and 1753.53 mm respectively.

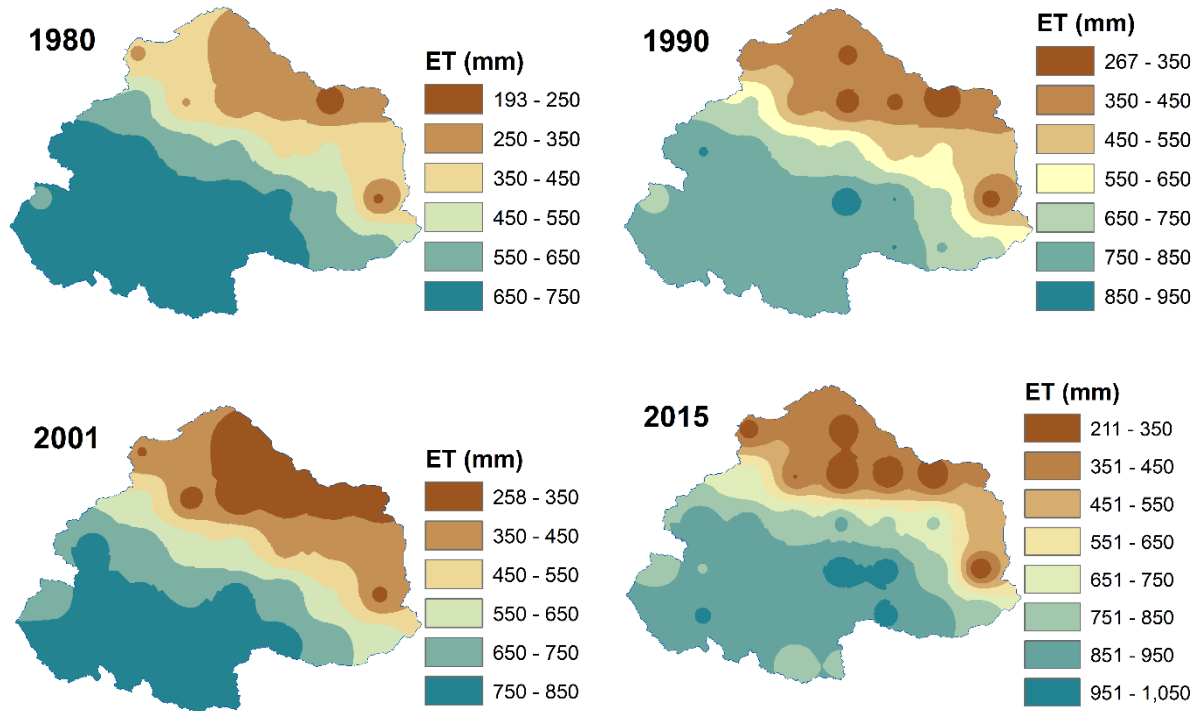


359

360 **Figure 7.** Water yield obtained by computing pixel wise value of parameter “w” from Donohue *et*
 361 *al.* (2012)

362 **5.2 Validation of ET and water yield estimates**

363 For validation purpose, the basin average annual values of PET and AET estimated using various
 364 strategies are compared with the corresponding basin average values obtained from available
 365 global datasets (Table 2). Model simulated AET values are obtained from GLDAS global ET
 366 datasets from Noah model outputs. Basin average values of PET dataset are obtained from Climate
 367 Research Unit (CRU) PET datasets (CRU TS v. 4.01) available at resolution of 0.5°. From the
 368 comparison, both AET (GLDAS) and PET (CRU TS) values are found to in agreement with the
 369 satellite estimated values. Spatial of Global datasets of AET and PET are shown in Figure 8 and
 370 9, respectively.

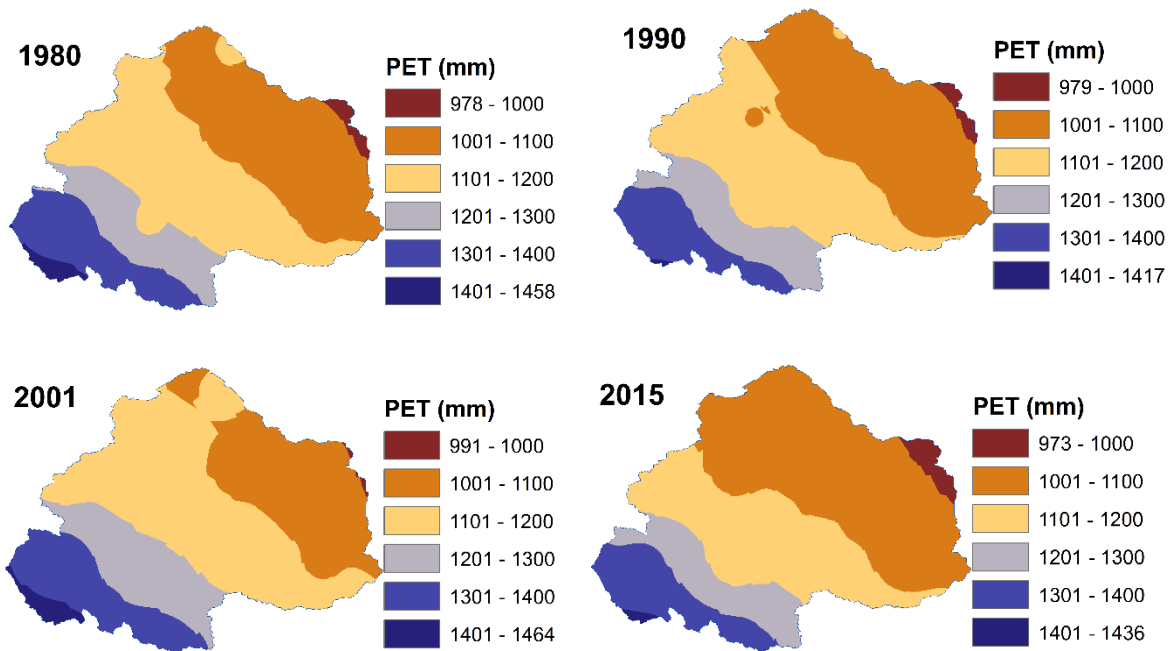


371

372

373 **Figure 8.** Spatial distribution of AET obtained from GLDAS Noah output datasets.

374



375

376

377 **Figure 9.** Spatial distribution of PET obtained from CRU datasets.

378

379

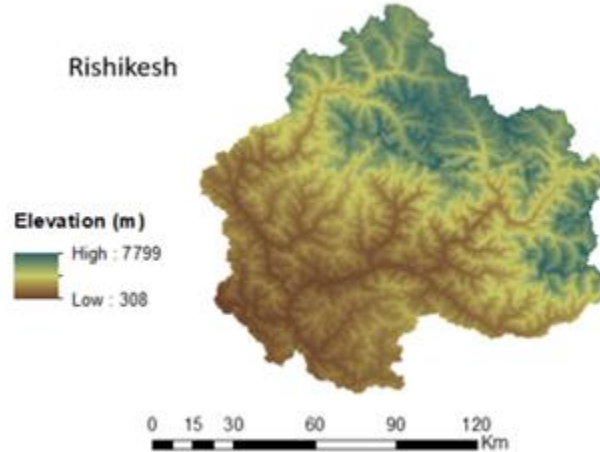
380 **Table 2:** Comparison of model estimated PET and AET with satellite estimates
 381

Parameter (mm)	Year	Source 2 (GLDAS)	Source 2 (CRU)	InVEST model				
				Strategy A (Lumped Zhang Model)	Strategy B (Large Model)	Strategy C (Global model)	Strategy D (Xu et al. 2013)	Strategy E (Donohue et al. 2012)
AET	1980	555.0355		696.84	486.07	679.52	679.68	680.01
	1990	646.168		815.02	592.3	735.23	735.27	736.25
	2001	588.084		680.76	408.86	548.28	548.39	550.38
	2015	716.8316		900.11	625.41	743.48	743.52	744.34
PET	1980		1175.964	1376.64	1382.12	1382.12	1382.12	1382.12
	1990		1156.497	1456.16	1461.86	1461.86	1461.86	1461.86
	2001		1184.847	1457.08	1462.96	1462.96	1462.96	1462.96
	2015		1156.686	1544.20	1550.42	1550.42	1550.42	1550.42

382

383 The validation of the water yield obtained from various strategies is performed upto Rishikesh
 384 gauging site of Upper Ganga basin (Fig. 10). The discharge data of the basin is obtained from
 385 Irrigation department of Uttarakhand state. Present work considers runoff from both precipitation
 386 as well as snowfall for the region, but 32% of the observed discharge has been removed as it is
 387 contributed by glacier ice melt to the streamflow for this catchment as explained by Maurya et al.
 388 (2011) for our study area. The above mentioned fraction of discharge had been quantified using
 389 isotope study which separates snow melt contribution from that of the glacier melt (Maurya et al.,
 390 2011). A comprehensive work on water balance of Upper Ganga Basin has been discussed by Jain
 391 et al. (2017) (Table 4 in Jain et al., 2017). For a precipitation value of 1236.1 mm, ground water
 392 contributes by an amount of 293.92 mm and snow melt contributes by 73.84 mm. It is apprehended
 393 that ground water flow and snow melt equals to 367.76 mm which is approximately equals to 29.75
 394 percent of Precipitation. Subsequently, this percentage contribution is also supported by the value

395 reported by Maurya et al. (2011). A comparison of the water yield computed and observed for the
 396 study region for different years by various proposed strategies are shown in Table 3.



397

398 **Figure 10.** Graphical representation of sub-basin Rishikesh

399 **Table 3.** Observed vs computed water yield by various proposed strategies for Rishikesh sub-
 400 basin.

Strategies	1980	1990	2001	2015
Observed discharge (mm)	1831.31	2422.43	2187.22	2835.81
Observed (mm) (after reducing approx. 32% snow melting contribution)	1245.29	1647.25	1487.31	1928.35
Water Yield_Strategy A (mm)	652.47	914.35	598.25	1189.72
Water Yield_Strategy B (mm)	745.38	917.77	697.75	1092.17
Water Yield_Strategy C (mm)	1229.90	1506.82	1102.62	1718.17
Water Yield_Strategy D (mm)	1229.99	1506.74	1102.61	1718.18
Water Yield_Strategy E (mm)	1230.77	1508.88	1106.86	1720.16

401

402 Values of water yield estimated using strategy A to E are systematically increasing but are not
403 steady in nature as water yield estimated using strategy A and B lies in range 650 – 750 mm
404 whereas water yield from strategy C-E lies in range 1229 – 1231 mm for the year 1980 (see Table
405 3). Similar results are also evident for other years too. Also, water yield estimated using strategy
406 C-E are more or less same for a given year as these strategies involve pixel based estimation of
407 water yield considering spatial variation in Budyko parameters. Parameters involved in Budyko
408 model such as ‘w’ are found to be dependent on various factors such as catchment characteristics,
409 vegetation cover, etc. as well as climate seasonality (Li et al. 2013). Ahn and Merwade (2017)
410 have analysed the relationship between basin characteristics and factor ‘w’ for 175 stations spread
411 over the USA results are presented in Ahn and Merwade, (2017). As evident from their study, no
412 precise conclusion can be drawn regarding relationship between basin characteristics and value of
413 ‘w’ especially in case of basin area characteristics. Moreover, no straight forward relationship has
414 yet been identified between basin characteristics and model parameters and it is a subject matter
415 for further study.

416 6. Discussion

417 The study aimed to apply the InVEST water yield model, a tool that is gaining interest in ecosystem
418 services community for Upper Ganga Basin, having the variability in the topography and
419 consisting of hilly areas, plain areas and the regions which are totally covered with snow. The
420 InVEST model is based upon Budyko theory which requires low amount of data and low level of
421 expertise, thus making it acceptable world-wide. Monthly precipitation, monthly average value of
422 temperature, monthly value of difference of mean daily maximum and mean daily minimum and
423 extraterrestrial radiation parameters are computed for the Upper Ganga Basin for each month of
424 all the four years i.e. 1980, 1990, 2001 and 2015 and converted into the raster format for the further

425 analysis. The monthly reference evapotranspiration is thus computed using input parameters in the
426 GIS environment by applying the modified Hargreaves equation for all the months except some
427 months where the modified Hargreaves equation shows the negative results for the reference
428 evapotranspiration value. For those months Hargreaves method is applied to obtain the positive
429 value of reference evapotranspiration as also suggested by Goyal et al. (2017). Reference
430 evapotranspiration when multiplied with K_c gives the potential evapotranspiration. All the monthly
431 values of different years are added up to obtain the yearly value of reference evapotranspiration.
432 K_c is the function of Land Use Land Cover, thus supervised classification is done to prepare the
433 raster Land Use Land Cover map for the Upper Ganga Basin. Thus, the yearly value of potential
434 evapotranspiration is obtained for the study area for the years 1980, 1990, 2001 and 2015.

435 The paper focuses on all the methodologies discussed in the paper and is applied on the Upper
436 Ganga basin. Thus, water yield is computed both from InVEST model as well as Lumped Zhang
437 model. The value of the parameter 'w' are computed in four ways, i.e. mean single value obtained
438 from Xu et al. (2013) for large basins and global model, pixel wise value of parameter 'w' from
439 Xu et al. (2013) and pixel wise value of parameter 'w' from Donohue et al. (2012). Although, the
440 Upper Ganga basin lies in large basin category as per the definition from Xu et al. (2013), but, the
441 yield computed using global model is in good agreement with the observed data for the Upper
442 Ganga basin. In the study, pixel level estimation of parameter 'w' is made in order to incorporate
443 the spatial variability of the parameter in water yield estimation. Thus, two pixel wise values of
444 parameter 'w' is computed for the Upper Ganga basin for years 1980, 1990, 2001 and 2015 by
445 considering two approaches as given by Xu et al. (2013) and Donohue et al. (2012). Also, the water
446 yield is computed from Lumped Zhang model which works on the approach of considering mean

447 values of all the parameters indulged in the computations of water yield. Thus, in five ways water
448 yield are computed for the Upper Ganga basin for the years 1980, 1990, 2001 and 2015.

449 At Rishikesh gauging site, surface runoff data is obtained by extracting the snow melt from the
450 discharge data as the snow melting contributes about 32 percent of total runoff (Maurya et al.,
451 2011). Using this fact, the observed yield is compared with the computed water yield based on
452 different proposed strategies for the years 1980, 1990, 2001 and 2015 represented in Table 3. The
453 results obtained from Donohue et al. (2012) and Xu et al. (2013) computed at pixel level (Strategy
454 C, Strategy D and Strategy E), thus represents better performance than other and are in good
455 agreement with the observed data. It is clear that in order to go for hydrological processing for any
456 watershed, pixel wise computation is advisable. The parameters involved in the Budyko model
457 are dependent on various factors such as basin characteristics (size, topography, stream length,
458 slope, etc.), climate seasonality, etc. (Li et al., 2013). The factors affecting model parameters again
459 vary both spatially and temporally. Moreover, the relationship between these factors and model
460 parameters are not yet well defined (Ahn and Merwade, 2017). In such scenario, adopting a
461 hypothesis by assuming few of these controlling factors (such as 'w') to be constant spatially or
462 temporally is inappropriate. Considering these facts, the present study attempts to incorporate the
463 spatial variability of model parameter for estimation of water yield at pixel level. As the
464 computations are made at pixel level in GIS environment, the assumption of dependence of model
465 parameters over scale of the catchment may also be disregarded. The computations made in present
466 work are based on empirical equations, however, the application of these equations has been well
467 documented worldwide for estimation of various water balance components at various basin scales
468 (Zhang et al., 2008; Ma et al., 2008; Ning et al., 2017; Rouholahnejad et al., 2017; Wang et al.,
469 2017). Hence, it is recommended, that for such a large basin there is a strong need to compute all

470 the parameters involved in the computations of water yield at pixel scale rather than adopting the
471 mean values for entire watershed.

472 **7. Summary and Conclusions**

473 The present study aimed to apply the InVEST annual water yield model, a tool that is gaining
474 interest in the ecosystem services community. While such simple models having low requirements
475 for data, high level of expertise are needed for practical applications of such model as a single
476 representative value of model parameter for the entire basin does not provide good estimates of
477 water yield. On the other hand, performing pixel scale computation of water yield indicates a better
478 performance and results obtained show better agreement with the observed water yield. As far as
479 parameter 'w' is concerned, global model works better than other representation of 'w' available
480 in literature. The water yield is computed using five different strategies and results are analyzed
481 with the observed data of sub-basins of Upper Ganga Basin. The present study attempts to quantify
482 annual water yield at pixel level irrespective of the size of catchment. Therefore, the proposed
483 methodology is expected to perform well for the catchment of any given size. Changes in
484 catchment's water storage over time are required to be quantified in order to validate the
485 applicability of Budyko's model to long term data for the catchment under study. Earlier, some
486 of the important parameters for the water yield used to be computed at a basin level scale which
487 brings noise in the results. Thus, by considering all the parameters involved in the model at pixel
488 level scale, the results obtained are higher in accuracy.

489 The study attempts to incorporate the spatial variability of parameters involved in the model
490 thorough pixel level estimation of parameters which are otherwise taken as lumped in the previous
491 studies. Study results show that the water yield estimated considering spatial variability in model
492 parameters are in better agreement with the observed water yield as compared to the water yield

493 estimated by considering the parameters to be lumped over the study region. Further, the
494 computations of various parameters are made at pixel level, therefore, the estimates of water
495 balance components using this approach are expected to be independent of the assumption of
496 dependence of parameters on catchment size. As the variation between Budyko's model
497 parameters and their controlling factors has not shown well defined relationship (Ahn and
498 Merwade, 2017), the study emphasizes water yield estimation using pixel based computations.
499 Thus it can be inferred that: (i) between two approaches used, i.e. considering entire basin and pixel
500 level approach, the pixel level approach is found to provide better results and (ii) in pixel level
501 based computations, results further improved with the use of a parameter 'w' based on a global
502 model than regional models of 'w' for large basins in Himalayan basin.

503 **Acknowledgement**

504 Authors are thankful to Executive Engineer, Irrigation Department, Uttarakhand, for providing the
505 discharge data for the Rishikesh sub-basin of Upper Ganga Basin.

506 **References**

507 Ahn, K. H., and Merwade, V. (2017). "The Integrated Impact of Basin Characteristics on Changes
508 in Hydrological Variables", Book Chapter 12 in "*Sustainable Water Resources Management*",
509 American Society of Civil Engineers (ASCE), pp. 317-336. ISBN: 978-0-7844-1476-7.

510 Allen, R. G., Pereira, L. S., Raes, D., and Smith, M. (1998). "Crop evapotranspiration-Guidelines
511 for computing crop water requirements"-FAO Irrigation and drainage paper 56. FAO, Rome,
512 300(9), D05109.

513 Bai, Y., Ouyang, Y., and Pang, J. S. (2012). "Biofuel supply chain design under competitive
514 agricultural land use and feedstock market equilibrium." *Energy Economics*, 34(5), 1623-1633.

515 Berghuijs, W. R., Woods, R. A., and Hrachowitz, M. (2014). “A precipitation shift from snow
516 towards rain leads to a decrease in streamflow.” *Nature Climate Change*, 4(7), 583-586.

517 Bharati, Luna, Guillaume Lacombe, Pabitra Gurung, Priyantha Jayakody, Chu Thai Hoanh, and
518 Vladimir Smakhtin (2011). *The impacts of water infrastructure and climate change on the*
519 *hydrology of the Upper Ganges River Basin*. Vol. 142. IWMI, 2011.

520 Budyko, M. (1958). *The Heat Balance of the Earth, Leningrad, 1956* (in Russian), Translation by
521 N. A. Stepanova, US Weather Bureau, Washington, p. 255.

522 Budyko, M. I. (1974). *Climate and Life*, Academic Press, New York, USA, 1-507.

523 Budyko, M. I., and Ronov, A. B. (1979). “Evolution of chemical composition of the atmosphere
524 during the Phanerozoic.” *Geokhimiya*, (5), 643-653.

525 Burkhard, B., Crossman, N., Nedkov, S., Petz, K., and Alkemade, R. (2013). “*Mapping and*
526 *modelling ecosystem services for science, policy and practice*. (4), 1-3.

527 Chen, X., Alimohammadi, N., and Wang, D. (2013). “Modeling interannual variability of seasonal
528 evaporation and storage change based on the extended Budyko framework.” *Water Resources*
529 *Research*, 49(9), 6067-6078.

530 Choudhury, B. (1999). “Evaluation of an empirical equation for annual evaporation using field
531 observations and results from a biophysical model.” *Journal of Hydrology*, 216(1), 99-110.

532 Donohue, R. J., Roderick, M. L., and McVicar, T. R. (2006). “On the importance of including
533 vegetation dynamics in Budyko’s hydrological model.” *Hydrology and Earth System Sciences*
534 *Discussions*, 3(4), 1517-1551.

535 Donohue, R. J., Roderick, M. L., and McVicar, T. R. (2012). “Roots, storms and soil pores:
536 Incorporating key ecohydrological processes into Budyko’s hydrological model.” *Journal of*
537 *Hydrology*, 436, 35-50.

538 Droogers, P., and Allen, R. G. (2002). “Estimating reference evapotranspiration under inaccurate
539 data conditions.” *Irrigation and drainage systems*, 16(1), 33-45.

540 Fu, B. P. (1981). “On the calculation of the evaporation from land surface.” *Sci. Atmos. Sin*, 5(1),
541 23-31.

542 Gentine, P., D’Odorico, P., Lintner, B. R., Sivandran, G., and Salvucci, G. (2012).
543 “Interdependence of climate, soil, and vegetation as constrained by the Budyko curve.”
544 *Geophysical Research Letters*, 39(19), L19404.

545 Goyal, M. K., and Khan, M. (2017). “Assessment of spatially explicit annual water-balance model
546 for Sutlej River Basin in eastern Himalayas and Tungabhadra River Basin in peninsular India.”
547 *Hydrology Research*, 48(2), 542-558.

548 Guswa, A. J., Brauman, K. A., Brown, C., Hamel, P., Keeler, B. L., and Sayre, S. S. (2014).
549 “Ecosystem services: Challenges and opportunities for hydrologic modeling to support decision
550 making.” *Water Resources Research*, 50(5), 4535-4544.

551 Hamel, P., and Guswa, A. J. (2014). “Uncertainty analysis of a spatially-explicit annual water-
552 balance model: case study of the Cape Fear catchment, NC.” *Hydrology and Earth System*
553 *Sciences*, 11, 11001-11036.

554 Hoyer, R., and Chang, H. (2014). “Assessment of freshwater ecosystem services in the Tualatin
555 and Yamhill basins under climate change and urbanization.” *Applied Geography*, 53, 402-416.

556 Jain, S. K., Jain, S. K., Jain, N., and Xu, C. Y. (2017). “Hydrologic modeling of a Himalayan
557 mountain basin by using the SWAT model.” *Hydrology and Earth System Sciences*,
558 <https://doi.org/10.5194/hess-2017-100>

559 Khatami, S., and Khazaei, B. (2014). “Benefits of GIS Application in Hydrological Modeling: A
560 Brief summary.” *VATTEN–Journal of Water Management and Research*, 70, 41-49.

561 Li, D., Pan, M., Cong, Z., Zhang, L., and Wood, E. (2013). “Vegetation control on water and
562 energy balance within the Budyko framework.” *Water Resources Research*, 49(2), 969-976.

563 Liston, G. E., and Elder, K. (2006). “A distributed snow-evolution modeling system
564 (SnowModel).” *Journal of Hydrometeorology*, 7(6), 1259-1276.

565 Ma, Z. M., S. Z. Kang, L. Zhang, L. Tong, and X. L. Su (2008). “Analysis of impacts of climate
566 variability and human activity on streamflow for a river basin in arid region of northwest China.”
567 *Journal of Hydrology*, 352(3–4), 239–249.

568 Maurya, A. S., Shah, M., Deshpande, R. D., Bhardwaj, R. M., Prasad, A., and Gupta, S. K. (2011).
569 “Hydrograph separation and precipitation source identification using stable water isotopes and
570 conductivity: River Ganga at Himalayan foothills.” *Hydrological Processes*, 25(10), 1521-1530.

571 McKenzie, N. J., Gallant, J., and Gregory, L. (2003). “*Estimating water storage capacities in soil*
572 *at catchment scales.*” CRC for Catchment Hydrology.

573 Mezentsev, V. (1955). “More on the computation of total evaporation (Yechio raz o rastchetie
574 srednevo summarnovo ispareniiia)” *Meteorog. i Gridrolog.*, 5, 24–26, 1955.

575 Milly, P. C. D. (1994). “Climate, soil water storage, and the average annual water balance.” *Water*
576 *Resources Research*, 30(7), 2143-2156.

577 Milly, P. C. D., and Dunne, K. A. (2002). “Macroscale water fluxes 2. Water and energy supply
578 control of their interannual variability.” *Water Resources Research*, 38(10), 241-249.

579 Nelson, E., Sander, H., Hawthorne, P., Conte, M., Ennaanay, D., Wolny, S., ... and Polasky, S.
580 (2010). “Projecting global land-use change and its effect on ecosystem service provision and
581 biodiversity with simple models.” *PloS one*, 5(12), E14327.

582 Ning, T., Li, Z., and Liu, W. (2017). “Vegetation dynamics and climate seasonality jointly control
583 the interannual catchment water balance in the Loess Plateau under the Budyko framework.”
584 *Hydrology and Earth System Sciences*, 21, 1515-1526

585 Ojha C.S.P., Bhunya P., and Berndtsson R. (2008). *Engineering Hydrology*, 1st Ed., Oxford
586 University Press, UK, 1-459.

587 Ol’Dekop, E. M. (1911). *On Evaporation from the Surface of River Basins*, Univ. of Tartu, Tartu,
588 Estonia, p. 209.

589 Pai, D. S., Sridhar, L., Rajeevan, M., Sreejith, O. P., Satbhai, N. S., and Mukhopadhyay, B. (2014).
590 “Development of a new high spatial resolution (0.25× 0.25) long period (1901–2010) daily gridded
591 rainfall data set over India and its comparison with existing data sets over the region.” *Mausam*,
592 65(1), 1-18.

593 Pike, J. G. (1964). “The estimation of annual run-off from meteorological data in a tropical
594 climate.” *Journal of Hydrology*, 2(2), 116-123.

595 Porporato, A., Daly, E., and Rodriguez-Iturbe, I. (2004). “Soil water balance and ecosystem
596 response to climate change.” *The American Naturalist*, 164(5), 625-632.

597 Potter, N. J., Zhang, L., Milly, P. C. D., McMahon, T. A., and Jakeman, A. J. (2005). “Effects of
598 rainfall seasonality and soil moisture capacity on mean annual water balance for Australian
599 catchments.” *Water Resources Research*, 41(6), 1-11.

600 Rouholahnejad Freund, E. and Kirchner, J. W. (2017). “A Budyko framework for estimating how
601 spatial heterogeneity and lateral moisture redistribution affect average evapotranspiration rates as
602 seen from the atmosphere.” *Hydrology and Earth System Sciences*, 21, 217-233

603 Sánchez-Canales, M., Benito, A. L., Passuello, A., Terrado, M., Ziv, G., Acuña, V., ... and Elorza,
604 F. J. (2012). “Sensitivity analysis of ecosystem service valuation in a Mediterranean watershed.”
605 *Science of the total environment*, 440, 140-153.

606 Schreiber, P. (1904). “Über die Beziehungen zwischen dem Niederschlag und der Wasserführung
607 der Flüsse in Mitteleuropa.” *Z. Meteorol*, 21(10), 441-452.

608 Shao, Q., Traylen, A., and Zhang, L. (2012). “Nonparametric method for estimating the effects of
609 climatic and catchment characteristics on mean annual evapotranspiration.” *Water Resources*
610 *Research*, 48(3), W03517.

611 Srivastava, A. K., Rajeevan, M., and Kshirsagar, S. R. (2009). “Development of a high resolution
612 daily gridded temperature data set (1969–2005) for the Indian region.” *Atmospheric Science*
613 *Letters*, 10(4), 249-254.

614 Su, C., and Fu, B. (2013). “Evolution of ecosystem services in the Chinese Loess Plateau under
615 climatic and land use changes.” *Global and Planetary Change*, 101, 119-128.

616 Tallis, H.T., Ricketts, T., Nelson, E., Ennaanay, D., Wolny, S., Olwero, N., Vigerstol, K.,
617 Pennington, D., Mendoza, G., Aukema, J. and Foster, J., (2010). *InVEST 1.004 beta User's Guide*.
618 The Natural Capital Project.

619 Terrado, M., Acuña, V., Ennaanay, D., Tallis, H., and Sabater, S. (2014). “Impact of climate
620 extremes on hydrological ecosystem services in a heavily humanized Mediterranean basin.”
621 *Ecological Indicators*, 37, 199-209.

622 Turc, L. (1954). “Le bilan d’eau des sols: relations entre les précipitations, l’évaporation et
623 l’écoulement.” *Annales Agronomiques A*, 20, 491–595.

624 Wang, D., and Tang, Y. (2014). “A one-parameter Budyko model for water balance captures
625 emergent behavior in darwinian hydrologic models.” *Geophysical Research Letters*, 41(13), 4569-
626 4577.

627 Wang, X.-S. and Zhou, Y. (2017). “Shift of annual water balance in the Budyko space for
628 catchments with groundwater-dependent evapotranspiration.” *Hydrology and Earth System
629 Sciences*, 20, 3673-3690

630 Williams, C. A., Reichstein, M., Buchmann, N., Baldocchi, D., Beer, C., Schwalm, C., ... and
631 Papale, D. (2012). “Climate and vegetation controls on the surface water balance: Synthesis of
632 evapotranspiration measured across a global network of flux towers.” *Water Resources Research*,
633 48(6), W06523.

634 Xu, X., Liu, W., Scanlon, B. R., Zhang, L., and Pan, M. (2013). “Local and global factors
635 controlling water-energy balances within the Budyko framework.” *Geophysical Research Letters*,
636 40(23), 6123-6129.

637 Yang, D., Sun, F., Liu, Z., Cong, Z., Ni, G., and Lei, Z. (2007). “Analyzing spatial and temporal
638 variability of annual water-energy balance in nonhumid regions of China using the Budyko
639 hypothesis.” *Water Resources Research*, 43(4), W04426.

640 Yang, H., Yang, D., Lei, Z., and Sun, F. (2008). “New analytical derivation of the mean annual
641 water-energy balance equation.” *Water Resources Research*, 44(3), W03410.

642 Zhang, L., Dawes, W. R., and Walker, G. R. (2001). “Response of mean annual evapotranspiration
643 to vegetation changes at catchment scale.” *Water resources research*, 37(3), 701-708.

644 Zhang, L., Hickel, K., Dawes, W. R., Chiew, F. H., Western, A. W., and Briggs, P. R. (2004). “A
645 rational function approach for estimating mean annual evapotranspiration.” *Water Resources
646 Research*, 40(2), W02502.

647 Zhang, L., N. Potter, K. Hickel, Y. Q. Zhang, and Q. X. Shao (2008). “Water balance modeling
648 over variable time scales based on the Budyko framework—Model development and testing.”
649 *Journal of Hydrology*, 360(1–4), 117–131.

650 Zhou, G., Wei, X., Chen, X., Zhou, P., Liu, X., Xiao, Y., ... and Su, Y. (2015). “Global pattern for
651 the effect of climate and land cover on water yield.” *Nature communications*, 6, 5918.

652 Zhou, S., Yu, B., Huang, Y., and Wang, G. (2015). “The complementary relationship and
653 generation of the Budyko functions.” *Geophysical Research Letters*, 42(6), 1781-1790.

654 Zhou, X., Zhang, Y., Wang, Y., Zhang, H., Vaze, J., Zhang, L., ... and Zhou, Y. (2012).
655 “Benchmarking global land surface models against the observed mean annual runoff from 150
656 large basins.” *Journal of Hydrology*, 470, 269-279.

657